Original
1-2
2/20/98

HUNTINGTON MEDICAL RESEARCH INSTITUTES
NEUROLOGICAL RESEARCH LABORATORY
734 Fairmount Avenue
Pasadena, California 91105

Contract No. NO1-NS-5-2333
QUARTERLY PROGRESS REPORT
October 1 - December 31, 1997

Report No. 9

"MICROSTIMULATION OF THE LUMBOSACRAL SPINAL CORD"

William F. Agnew, Ph.D.
Randy R. Carter, Ph.D.
Albert Lossinsky, Ph.D.
Douglas B. McCreery, Ph.D.
Leo A. Bullara, B.A.

Abstract

In this report, we discuss the results of one chronic and three acute experiments. We also present data from preliminary high-voltage electron microscopic studies of a chronically implanted pulsed electrode from a previous animal.

The animal with the chronically-implanted arrays demonstrated variability in the location of individual electrodes as a result of the electrodes having bent during implantation. Consequently, this animal presented histologic features related to movement of the electrodes. Considerable compression of the spinal cord was observed and may have been due to compression of the cord after closure of the dura. Within the capsules surrounding the electrodes and their tips, we observed fibrosis, hemorrhagic scarring, and a leukocyte infiltration composed primarily of lymphocytes along the entire length of some of the electrode tracks. The final electrode positions suggested they followed diverging paths as they penetrated the spinal cord. These electrodes were 24 μm in diameter. We had hoped these thinner electrodes would inflict less tissue injury, but apparently, they were too flexible. In the next arrays, we will increase the diameter of the electrodes to 34 μm.

The acute animal experiments showed the typical histologic spectrum seen in acute traumatic spinal cord injury including disruption of the angioarchitecture leading to damage of the *blood-spinal cord barrier and an edematous neuropil with associated neuronal shrinkage and glial swelling. One of the acute animals was perfused with a fixative that is compatible with immunocytochemical studies and the tissue was embedded in paraffin. We were able to successfully evaluate the electrode tracks and the sites of the electrode tips in the thicker 8 μm H & E-stained sections. The tissue processing was completed within two weeks, a significant improvement over the usual 4-6 weeks required for evaluation of plastic sections. Finally,*

analytical electron microscopy performed on one chronically-implanted pulsed electrode suggested exfoliation of iridium into the tissue capsule surrounding the electrode tip.

Introduction

The overall goals of this contract are to develop a method of chronic microstimulation of the sacral cord of the cat to effect micturition, and to evaluate the effects of the electrical stimulation on neural elements and other cells. In this report we discuss the results from one chronic experiment in which two arrays of three iridium microelectrodes were implanted in the spinal cord for 56 days. Previous studies indicated that smaller electrode shaft diameters induced less mechanical damage to the spinal cord as determined from its number of microhemorrhages and the severity of neuronal and axonal damage. However, histologic analysis indicated that the thin electrode shafts bent during insertion, a clearly undesirable result.

In the past, our process of evaluation and array design has suffered somewhat due to a slow turn around time for histologic analysis. Efforts were made in this quarter to correct this by moving to a paraffin embedding technique. This has reduced the time required for histologic analysis by as much as one-half.

Methods

Chronic experiments. One adult male cat was anesthetized with 50% nitrous oxide and 1-2% Halothane and the spinal cord exposed as described previously. The S_2 region of the spinal cord was localized by stimulation of the dermatome it serves while recording the dorsal cord potential supradurally. Two arrays of three activated iridium microelectrodes (24 μm dia., 2.8 mm long, 2000 μm^2 exposed stimulating surface) extending from a solid epoxy matrix were implanted manually at approximately the dorsal root entry zone of the spinal cord. The center electrode was pulsed during insertion and the bladder lumen pressure was monitored. Each array was advanced into the cord until elevation of bladder pressure was produced by the stimulation. The dura was then closed over the electrodes and the effect of the stimulation was measured again. A silastic pad (to which the leads of the array had been glued) was sutured to the dura to reduce traction on the electrodes. The ground (indifferent) electrode was sutured in place over the arrays. A small hole was made in the dura and a recording electrode inserted so as to lie approximately 3 cm caudal to the stimulating electrodes. A suture was used to secure the recording electrode to the dura. A reference electrode, placed above the dura but within the vertebral canal, was passed caudally about 3 cm and sutured to the dura. The wound was flushed with antibacterial solution and the muscle and skin were closed

in layers. Subsequent recordings were made with the animal anesthetized with Pentothal (i.v., as needed) or Nembutal (i.v., as needed). A sterile catheter and sterile saline were used during recording of the bladder lumenal pressure.

Acute experiments. Two adult male cats were anesthetized with 50% nitrous oxide and 1-2% Halothane. The spinal cord was exposed using a standard dorsal laminectomy and the rostral extent of the S_2 region was localized in the manner described above. Manually inserted microelectrodes were used to penetrate the spinal cord several times as a model of acute trauma.

A novel electrode array was tested in one acute animal experiment (SP-87), in which standard 7-0 suture needles bent into a semicircle were used as introducers to pull lengths of one or more insulated lead wires through the spinal cord. The leads were swedged onto the needles and were composed of either: 1) a single 50 μm diameter gold wire or 2) one, two, or three 25 μm diameter annealed platinum wires. The material from the acutely injured S_1-$_2$ spinal cords of these animals: 1) serves as cytochemical and immunocytochemical control tissue, 2) provides the first evaluations of a novel electrode as described in detail below, and 3) serves to evaluate paraffin embedding as a means of assessing mechanically induced tissue injury.

Histology.

Experiment	**Time Duration Between Electrode Implanting And Fixation**
SP-83	3 Hours
SP-84	3 Hours
SP-85	56 Days
SP-87	3 Hours
SP-77	31 Days

TABLE 1

TABLE 1 presents the time between electrode insertion and perfusion. Within 20 minutes after the end of each experiment, the animals were anesthetized with Nembutal and perfused through the aorta with either: 1) phosphate-buffered saline followed by 4 L of ½ strength Karnovsky's fixative (2%

formalin and 2.5% glutaraldehyde) in 0.1 M sodium cacodylate buffer, pH 7.4 at 25°C, or 2) Ringers solution followed by 4% formalin and 0.1% glutaraldehyde in 0.1 M sodium cacodylate buffer, pH 7.4 at 25°C. The animals were stored in a refrigerated cold room until necroscopic examinations were performed, usually 24-48 hours after perfusion or, in the case of tissue for immunocytochemistry, within 2-3 hours after perfusion. With the electrodes ***in situ***, the complete cord and spinal roots were dissected out to precisely localize the microelectrodes. Spinal cord (S_{1-2}) sections containing the electrode tracks were dissected, processed, and embedded in plastic or paraffin.

A portion of the electrode capsule near the tip of pulsed electrode #4 (SP-77) was selected for elemental using high-voltage electron microscopic analysis. 0.5-1.0 μm plastic sections were collected on formvar-coated slot grids, stained with lead and uranyl salts and examined at the Wadsworth Laboratory of the New York State Department of Health in Albany with Dr. Bill Tivol (a two day satellite trip to Albany, NY from Bethesda, MD by Dr. Lossinsky on October 20-21, 1997).

Spinal Cord Model. A model of the feline spinal cord was cast from a viscous agar solution poured into a mold approximating the size and shape of the feline lumbosacral cord. When cooled to room temperature, this agar also demonstrated mechanical properties quite similar to the normal living spinal cord. The transparency of the model allowed us to examine the path of electrodes of various diameters during insertion.

Results

Arrays of three 24 μm diameter electrodes were inserted into the spinal cord model (agar mold) while observing their penetration pattern through a surgical microscope. This confirmed that due to slight misalignments, the electrodes often followed divergent paths upon entry. This was then repeated using 34 μm diameter electrodes. The 34 μm electrodes did not appear to bend during insertion.

Comparative histologic analyses were performed on four animals and tissue for elemental analysis was taken from a single electrode from a fifth animal. In two acute cats (SP-83, SP-84), single iridium electrodes (34 μm in diameter) were inserted repeatedly into the spinal cord. Histologic studies of these animals demonstrated morphological evidence of acute traumatic injury.

Findings in the acute animals were similar to those which have been reported in our previous QPRs, including massive hemorrhage occupying a large portion of approximately one half of the cord and consisting of numerous erythrocytes, leukocytes and plasma proteins within the neuropil, due to rupture of the blood-spinal cord barrier. The extracellular space was locally swollen (massive vasogenic edema), and selective injury to some neurons was observed including chromatolysis and shrinkage, as well as swelling of glial cells within the tissue immediately surrounding the electrode tracks (Fig. 1a-c).

In SP-85, the dorsal surface of the S_2 spinal cord appeared compressed, presumably from the downward pressure produced by closing (suturing) the dura directly over the solid epoxy matrix of the multiple electrode array (Fig 2). We also noticed an unusual relationship of the 24 μm electrodes in the three electrode array assemblies. On gross inspection during necroscopy, two of the six implanted electrodes (#4 and #6) were observed extending from the S_2 segment of the spinal cord. Four electrodes and their tips were located within the spinal cord. The locations of electrodes #1, 2 and 3 within the tissue suggested that the three electrodes diverged during implantation, possibly due to their excessive flexibility. For this reason, the precise identity of the electrodes in SP-85 remains equivocal. Other observed changes include gliosis, vascular hypertrophy and hyperplasia in the vicinity of the electrode tracks, and selective perivascular cuffing associated with inflammatory foci (Figs. 3a,b). One electrode also traumatized the central canal, leading to marked edematous changes in the surrounding neuropil (Fig. 3c). The scarring adjacent to some of the electrodes was suggestive of electrode movement.

In SP-87, curved needles trailing one or more lead wires were passed through the cord in a rostro-caudal direction. In one case the needle crossed the midline of the cord rather than remaining unilateral, as intended. In all other cases, it was possible to insert the needles through the cord by pushing them in and then pulling out the tip in very small steps. In this way, the needle followed a path determined by its curvature. The lead wires were drawn into the cord along the same course. An advantage of this approach is that after the introduction needle is removed, the wires can be pulled from either end without cutting through the tissue. A deinsulated region could act as a stimulation site which could be repositioned without a subsequent penetration of the spinal cord. If multiple wires are passed through the cord in this manner, it is possible to position each independently.

We observed several acute tissue changes associated with the insertion of the needle introducers and their leads as they were pulled into position within the spinal cord. Many of the changes were similar to those of other acute animals in which the tissue was embedded in plastic (SP-83 and SP-84) including edema with hemorrhage. There was an inflammatory response within the pial blood vessels three hours after the injury. The tips of the three electrodes from the linear array were positioned similarly within the ventral gray horn (Fig. 4a-c).

Tissue obtained near the tip of pulsed electrode #4 from SP-77 was examined by high-voltage electron microscopy (Fig. 5a). Elemental analysis of the dense particulate material within the tissue capsule surrounding the tip of this electrode indicated metallic iridium (Fig. 5b). This animal was post-fixed with osmium tetroxide and the thick-sections were stained with conventional lead and uranyl stains to improve the contrast of the cellular membranes.

Discussion

The implantation of multiple wire electrodes into the spinal cord by a curved needle introducer shows some promise. The insertion was not difficult or time consuming and each wire could be moved back and forth independently. Thus, a deinsulated stimulating region could be repositioned after insertion. We are currently developing techniques to seal these leads after the introducer wire is cut away. It may also be possible to use such a technique to place a stop at the point of the lead's ingress and egress thus stabilizing the position of the stimulating site. However, the passage of the needle through the cord did inflict considerable injury, and the trajectory of the needle was rather difficult to control. Smaller needles (such as those used with for 9-0 or 10-0 suture) may inflict less injury.

We originally favored the smaller 24 μm discrete iridium electrodes because of the reduced tissue scarring. However, the results from SP-85 and the tests using the spinal cord agar mold model suggest that the thinner electrodes may bend and diverge during implantation. Thus, increasing the diameter of the electrodes from 24 μm to 34 μm may improve the performance of the three electrode array since we observed that the tips of all three electrodes were in the target locations in SP-87 (Fig. 4). Although increasing the diameter of the electrodes to 34 μm may produce slightly more tissue injury during electrode implantation, we feel that improved electrode stability will prevent undesirable electrode movement and additional tissue injury during long-term residence in the cord.

The change in embedding medium reduced the processing time by about 50%. Although some future experiments will employ plastic embedding because it will be crucial to perform ultrastructural assessments of the material, paraffin embedding will be used for routine histologic evaluation in future experiments. Moreover, it provides us with a practical and realistic approach for detailed immunocytochemical studies. Whether or not the appearance of inflammatory cells is related exclusively to pulsed electrodes is an important question that we will address in future experiments. Finally, the iridium metal that exfoliated from a pulsed spinal cord electrode is similar to that which has been previously documented in cat brain tissue by our group (Tivol et al., 1987).

Future Work

Based on the results of the experiments in this quarter, we have decided to: 1) return to the use of larger diameter electrodes to improve their stability during implantation, and 2) begin using paraffin embedding as our standard technique to expedite tissue analysis. We also plan to pay particular attention to inflammatory cell infiltrates using antibodies produced against several known leukocyte CD antigens to evaluate a possible correlation between leukocyte presence and the pulsing of electrodes. We will also continue to evaluate metal deposition from electrodes during chronic electrical stimulation. The elemental analysis of the tissue adjacent to the pulsed electrode from SP-77 establishes the framework for further studies, especially in tissue that will be prepared without post-fixation with osmium tetroxide and lead staining. In this way, we will be able to identify iridium deposits within the tissue capsule without altering the true elemental spectrum partially masked by metallic osmium and lead, shown in Fig. 5.

References

Tivol, WF, Agnew, WF, Alvarez, RB, and Yuen, TGH (1987) Characterization of electrode dissolution products on the high voltage electron microscope. *J. Neurosci. Meth.* **19**: 323-337.

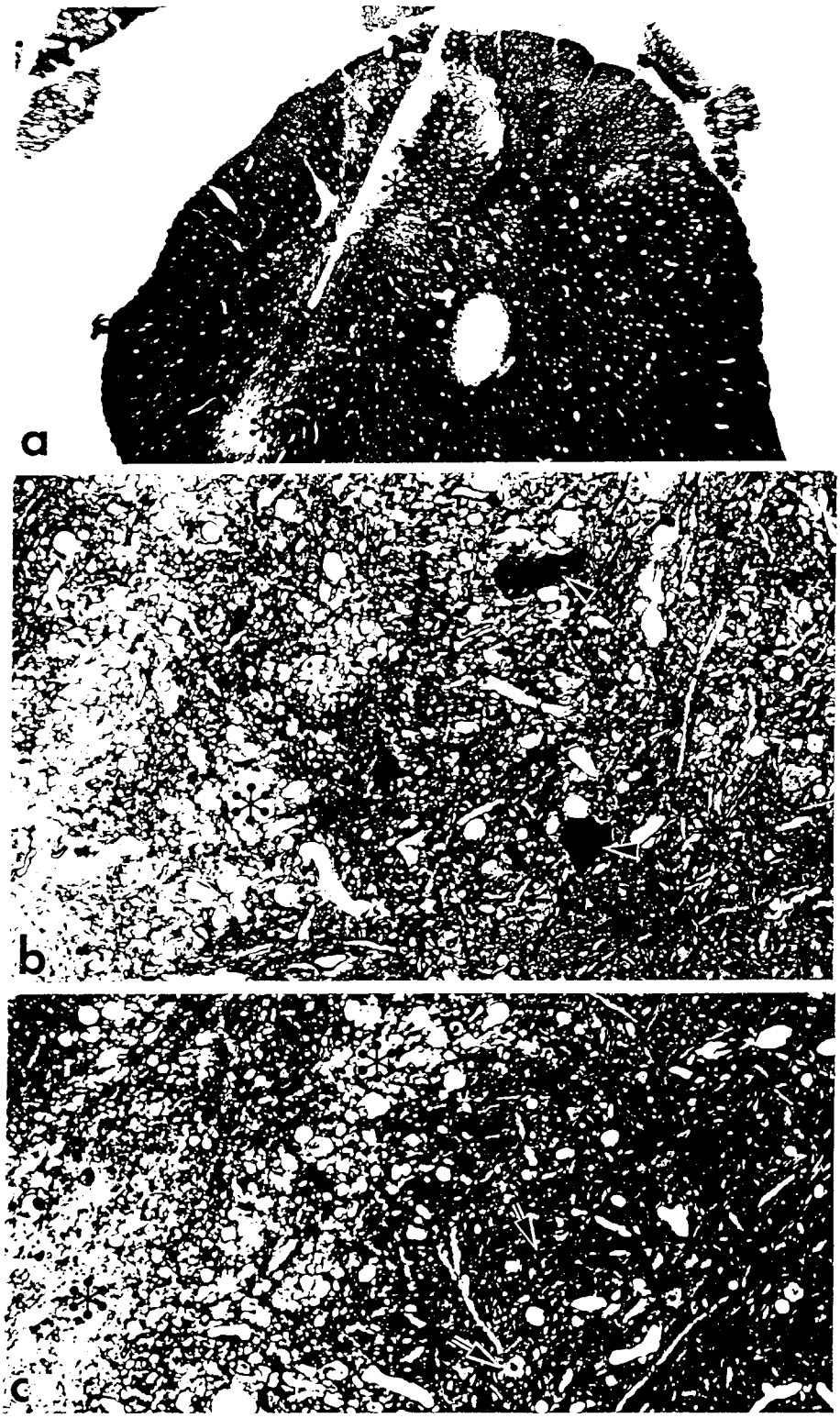

Fig. 1. SP-84, S_2 region shows some of the histopathologic changes in the acute animals. Inserting the electrodes several times into the spinal cord produces trauma including massive edema (a, b, c *), darkening of some neurons in areas adjacent to the electrode track (b, arrowheads), while other neurons appear normal (c, arrows). One μm plastic section. Bars = a: 400 μm; b: 50 μm; c: 50 μm.

Fig. 2. SP-85 demonstrates the compression of the dorsal right side of the S_2 spinal cord produced by the epoxy matrix portion of the chronically implanted multiple electrode array. Note the areas of edema produced by the electrode (*). One μm plastic section. Bar = 400 μm.

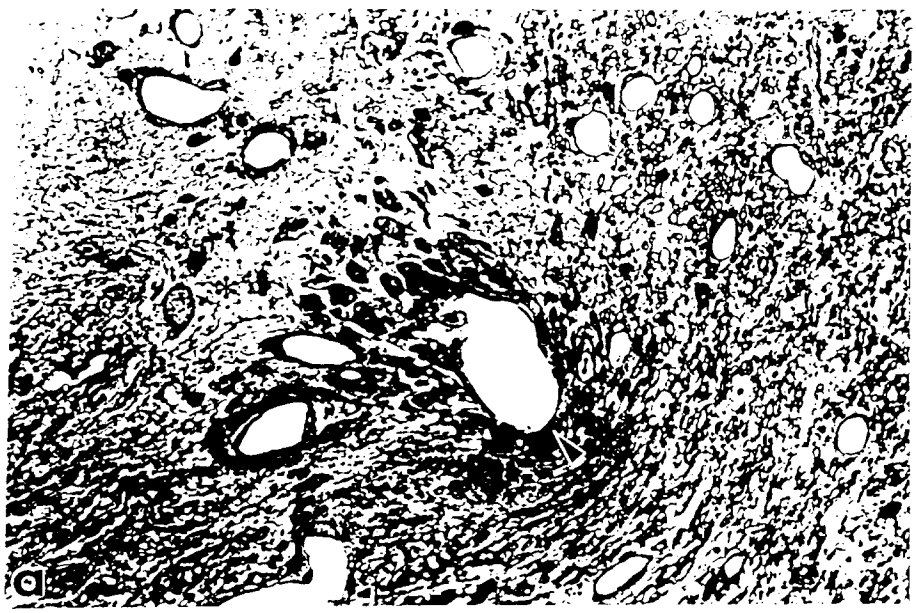

Fig. 3a. SP-85. Tissue is shown surrounding an electrode positioned at the border between the ventral gray horn and the white matter. A thin capsule is shown surrounding the electrode near its tip (arrowhead). Pathologic changes seen in the pericapsular region include fibrotic changes (*), reactive astrocytes, phagocytic cells, few lymphocytes and vessel hyperplasia. One μm thick plastic section. Bar = 25 μm.

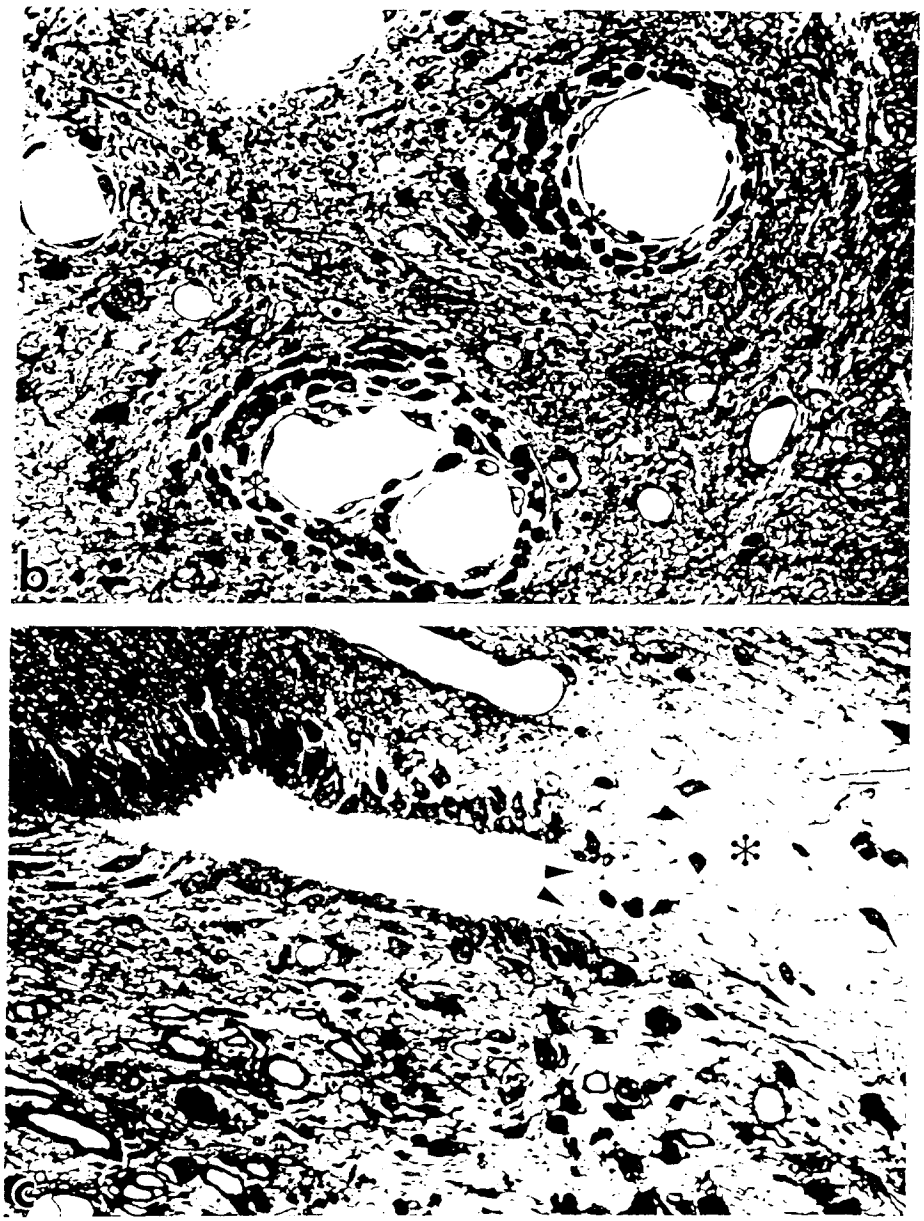

Fig. 3b, c. SP-85. b. Perivascular cuffing around some but not all vessels is shown(*). The leukocytes that comprise these cuffs include primarily small lymphocytes and few mononuclear cells. c. This figure demonstrates a severely edematous neuropil (*) produced by its traumatized ependymal cell layer surrounding the spinal cord's central canal (arrowheads). Cerebrospinal fluid infiltrates the surrounding neuropil because of the frank rupture of the ependymal cell layer. One μm thick plastic sections. Bars = b: 25 μm; c: 25 μm.

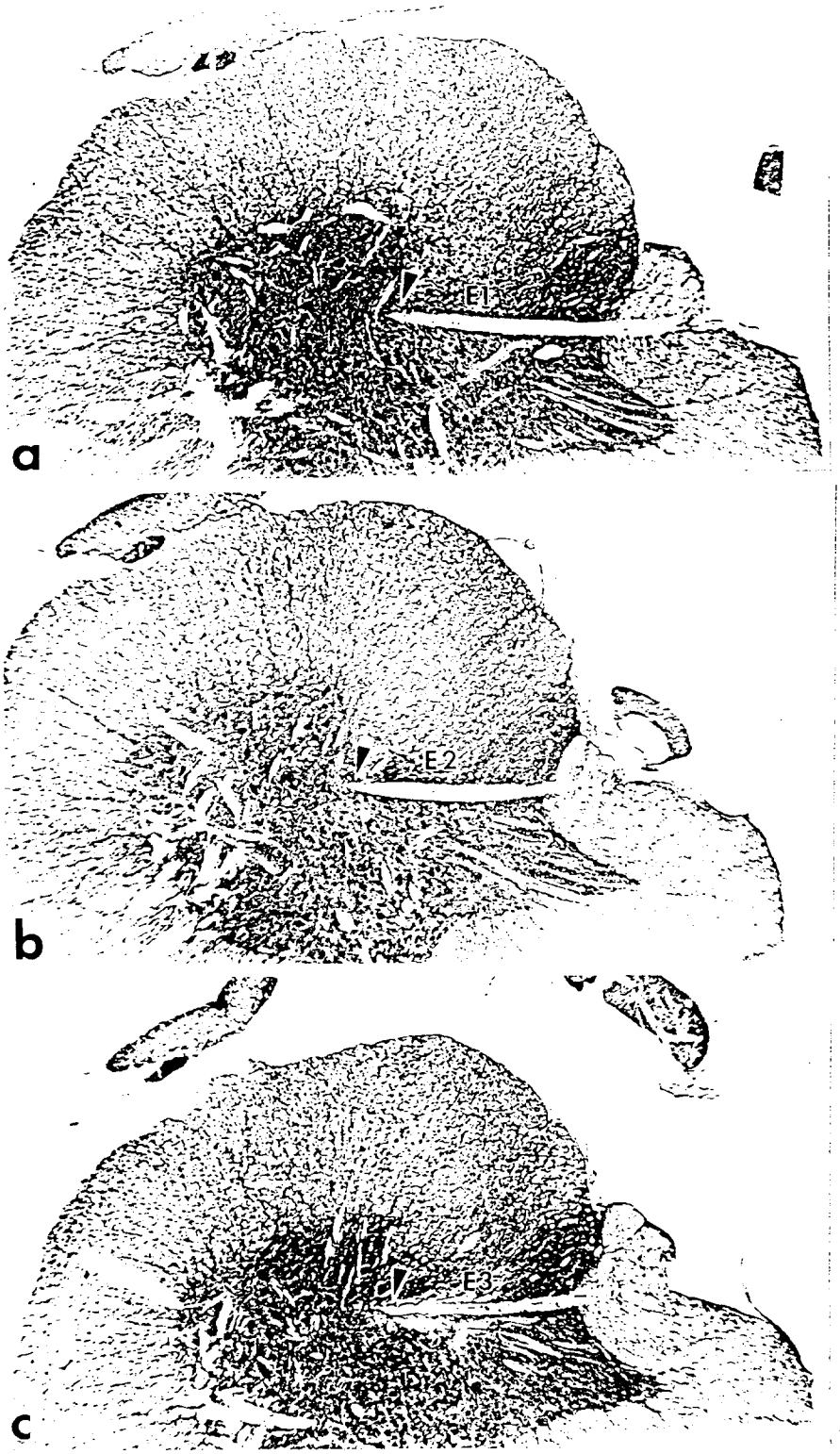

Fig. 4a-c. SP-87, lumbar spinal cord. These micrographs present the positioning of the three 34 μm diameter electrodes comprising the array. The cat was perfused 3 hrs after implanting the array. Note that all electrode tips (arrowheads) were well positioned within the ventral gray horn. Eight μm thick paraffin sections. Bars a-c = 400 μm.

a

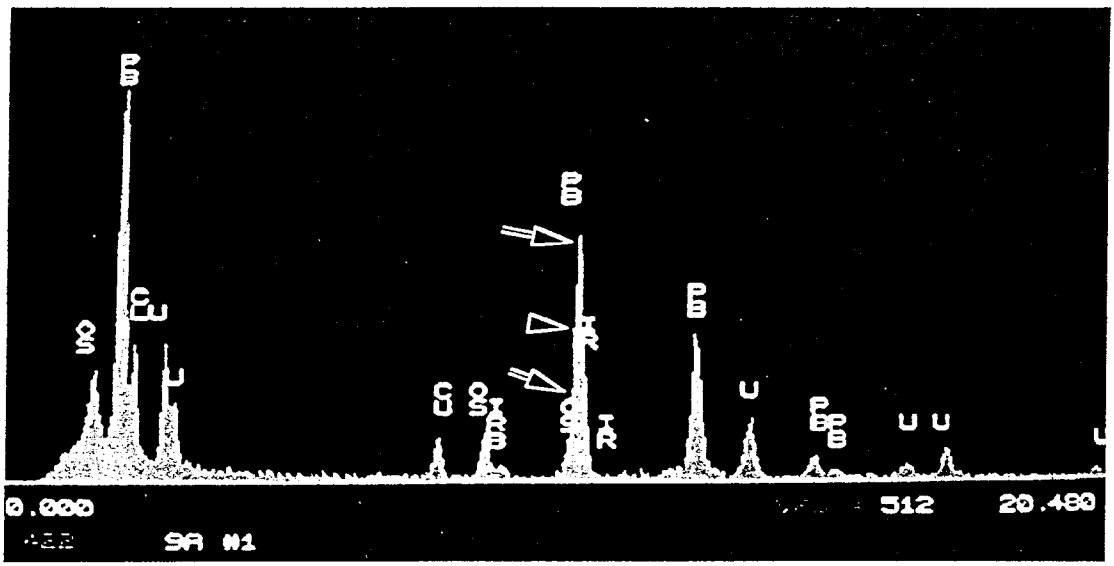

b

Fig. 5. a. SP-77. High-voltage electron microscopic stereo pair images show precipitate material located within the capsule at the tip of a pulsed electrode. Three-dimensional image can be observed with or without the aid of a stereo lens. Note the laminated striations of the metal deposits demonstrating the striated nature of this material. b. Analysis of the precipitate in Figure 5a. suggests the presence of iridium within this material and shows that the peak of iridium (arrowhead) overlaps with metallic lead (long arrow) and osmium (short arrow).